



HAL
open science

A novel TMPRSS6 mutation that prevents protease auto-activation causes IRIDA.

Sandro Altamura, Flavia d'Alessio, Barbara Selle, Martina Muckenthaler

► To cite this version:

Sandro Altamura, Flavia d'Alessio, Barbara Selle, Martina Muckenthaler. A novel TMPRSS6 mutation that prevents protease auto-activation causes IRIDA.. *Biochemical Journal*, 2010, 431 (3), pp.363-371. 10.1042/BJ20100668 . hal-00525044

HAL Id: hal-00525044

<https://hal.science/hal-00525044>

Submitted on 11 Oct 2010

HAL is a multi-disciplinary open access archive for the deposit and dissemination of scientific research documents, whether they are published or not. The documents may come from teaching and research institutions in France or abroad, or from public or private research centers.

L'archive ouverte pluridisciplinaire **HAL**, est destinée au dépôt et à la diffusion de documents scientifiques de niveau recherche, publiés ou non, émanant des établissements d'enseignement et de recherche français ou étrangers, des laboratoires publics ou privés.

A novel TMPRSS6 mutation that prevents protease auto-activation causes IRIDA.

Sandro Altamura^{1,2}, Flavia D'Alessio^{1,2,3}, Barbara Selle^{4,5}, Martina U. Muckenthaler^{1,2,5}

¹Department of Pediatric Oncology, Haematology and Immunology, University Hospital of Heidelberg; Germany, ²MMPU - Molecular Medicine Partnership Unit, Heidelberg, Germany, ³EMBL - European Molecular Biology Laboratory, Heidelberg, Germany, ⁴Helios Klinikum, Berlin, Germany, ⁵these authors contributed equally to this work

Abstract

IRIDA (Iron-Refractory Iron Deficiency Anemia) is a rare, autosomal recessive disorder hallmarked by hypochromic, microcytic anemia, low transferrin saturation and high levels of the iron-regulated hormone hepcidin. The disease is caused by mutations in the transmembrane serine-protease *TMPRSS6* that prevent inactivation of Hemojuvelin (HJV), an activator of hepcidin transcription. Here we report a patient with IRIDA that carries a novel mutation (Y141C) in the SEA domain of the *TMPRSS6* gene. Functional characterization of the *TMPRSS6*(Y141C) mutant protein in cultured cells shows that it localizes to similar subcellular compartments like wild-type *TMPRSS6*, binds HJV and but fails to auto-catalytically activate itself. As a consequence, hepcidin mRNA expression is increased causing the clinical symptoms observed in this IRIDA patient. This study yields important mechanistic insight into how *TMPRSS6* is activated.

Keywords: IRIDA, *TMPRSS6*, matriptase-2, Hpcidin, hemojuvelin.

Corresponding author: M.U. Muckenthaler, Im Neuenheimer Feld 156, Heidelberg – Germany. Fax: +49 6221 564580, Email: martina.muckenthaler@med.uni-heidelberg.de

Introduction

Patients with Iron-Refractory Iron Deficiency Anemia (IRIDA) absorb insufficient amounts of iron from the diet and respond inadequately to oral ferrous sulphate therapy and intramuscular iron dextran injection [1]. As a consequence iron-deficiency anemia develops that is characterized by hypochromic, microcytic erythrocytes and low transferrin saturation. IRIDA is usually diagnosed by routine haematological screening during childhood. Frequently, the affected subjects do not show the typical clinical symptoms of iron deficiency; pallor, dry skin or lesions at the corners of the mouth have been reported in only few cases [2-4]. IRIDA is a rare, autosomal recessive disorder [5] mapped to chromosome 22 (22q12.3-13.2) [2], which contains *TMPRSS6* (Transmembrane protease serine 6, also known as Matriptase-2) the gene responsible for IRIDA [6]. *Tmprss6* was initially characterized in the *mask* mouse, in which chemically induced mutations resulted in the loss of the *Tmprss6* protease domain. Similar to IRIDA patients and *TMPRSS6*^{-/-} mice [7], the mouse model is hallmarked by microcytic anemia due to ineffective dietary iron absorption [8].

TMPRSS6 is a member of the type II transmembrane serine protease family (TTSP) and is mainly expressed in the liver [9]. Similar to other TTSP members, *TMPRSS6* consists of a short N-terminal intracytoplasmic tail, a type II transmembrane domain, a stem region composed of two extracellular CUB (Complement factor C1s/C1r, Urchin embryonic growth factor, Bone morphogenetic protein) domains and 3 LDLR (Low-Density-Lipoprotein Receptor class A) domains and a C-terminal trypsin-like serine protease domain [9]. Between the transmembrane domain and the stem region there is a low homology SEA (Sea urchin sperm protein, Enteropeptidase, Agrin) domain [10]. *TMPRSS6* is rich in post-translational modifications. Consensus sites for N-glycosylation are located within the SEA domain, the second CUB domain and within the second LDLR domain [11]. 37 evolutionary conserved extracellular cysteines located within the CUB, the LDLR and the protease domains are at least partially involved in the formation of disulfide bridges [11]. *In silico* analysis of the human *TMPRSS6* revealed a possible phosphorylation site within the intracytoplasmic tail which was hypothesized to be involved in signal transduction. [9]. *TMPRSS6* is produced as a zymogen, a single chain inactive proenzyme, which auto-activates itself by cleavage at an arginine residue at the consensus site RIVGG between the prodomain and the catalytic domain. The activated catalytic domain remains attached to the rest of the protein at the cell surface via a single disulfide bridge [9].

Functionally, *TMPRSS6* has been linked to the hepatic iron sensing pathway by the observation that hepcidin levels are strongly increased in IRIDA patients and *TMPRSS6* mutant mice [2, 6, 8]. Hepcidin is a small peptide hormone produced by the liver in response to iron levels, inflammatory signals, hypoxia and the erythropoietic drive. Hepcidin controls systemic iron fluxes by binding to the iron exporter ferroportin inducing its internalization and degradation [12]. Thus, high hepcidin levels, as observed in IRIDA, inhibit intestinal iron absorption and macrophage iron release.

Under physiological conditions *TMPRSS6* down regulates hepcidin levels by binding and proteolytically degrading the hepcidin activator and BMP co-receptor hemojuvelin (HJV), a protein mutated in hereditary hemochromatosis type 2 [13]. *TMPRSS6* mutations that decrease its proteolytic activity and prevent HJV cleavage cause increased hepcidin levels that impair iron release from the duodenal enterocytes and macrophages [13]. *TMPRSS6* mutations linked to IRIDA are detected throughout the *TMPRSS6* gene. These include missense, nonsense, frameshift and splice junction mutations [14]. Missense mutations are predominantly located in the CUB (G442R), LDLR (D521N, E522K) and protease (L674F, R774C) domains. Only a single mutation so far has been reported in the SEA domain (A118D) [15].

Here we report a novel homozygous missense mutation (c.422A>G) in the fourth exon of *TMPRSS6* that substitutes tyrosine with cysteine at aminoacid 141. Interestingly, this mutation located in the SEA domain, abolishes *TMPRSS6* autocatalytic activation causing an increase of hepcidin levels and the characteristic IRIDA phenotype. Together with a previous report [15] our

finding suggests that the SEA domain plays an essential role in TMPRSS6 maturation and yields new insights into the proteolytic activation mechanism of this TTSP family member.

Materials and methods:

Urinary hepcidin analysis

Hepcidin analysis was essentially performed as described, previously [16]. Briefly, morning urine from the patient and from four age- and sex-matched healthy volunteers was centrifuged for 5 minutes at 3000g. 7 µl supernatant and 3 µl ammonium acetate buffer (0.1M; pH6) were mixed, incubated for 5 minutes at RT and directly applied to a pre-activated CM10 ProteinChip. Following 30 minutes of incubation in a humid chamber, the CM10 strip was washed 3 times with 30mM ammonium acetate (pH=6) and air-dried. 1 µl of Sinapic acid (SPA) was added onto each spot, air dried and reapplied. ProteinChips were read using a PBS IIc SELDI mass spectrometer (Bio-Rad – Hercules, CA) pre-calibrated with a standard reference including synthetic hepcidin. Data acquisition parameters were set up to the following: high mass 50000 Daltons, mass optimization from 1500 to 10000 Daltons, laser intensity 180, detector sensitivity 9, mass deflector 1500 Daltons, 2 warming shots at intensity 185 (without warming shot collection), acquisition of 50 shots every 5 positions from 27 to 87.

Data analysis was performed using the Ciphergen ProteinChip® Software Version 3.2. Hepcidin levels, measured as arbitrary intensity units, were normalized against creatinine values obtained from the same samples (Analysezentrum of the University Clinic of Heidelberg – Germany). All samples were spotted and analyzed in triplicate.

Patient clinical analysis

Informed consent was obtained from the parents of the patient and the healthy volunteers according to German law. Hematological parameters were measured at the “Zentrum für Kinder- und Jugendmedizin, St. Annastift, Ludwigshafen – Germany”. The iron-related values (ferritin, transferrin, transferrin saturation, serum transferrin receptor, free serum iron, iron binding capacity, zinc-protoporphyrin, haptoglobin, erythropoietin) were measured at the Prof. Seelig Laboratories, Karlsruhe – Germany. Patient DNA was extracted from peripheral blood by using the Qiagen DNeasy blood and tissue kit. Exons 1-18 of the TMPRSS6 gene were amplified by PCR using Platinum Taq DNA Polymerase (Invitrogen) and previously published primer pairs [6]. Sequencing was performed by GATC-biotech (GATC biotech, Konstanz, CH). Chromatograms were visualized with FinchTV (Geospiza) and analyzed with SeqMan (DNASTAR). ALAS2 (exons 1-10), SLC25A28 (exons 1-4), SLC11A2 (exons 2-16) were PCR amplified and sequenced at the Prof. Seelig Laboratories, Karlsruhe – Germany.

Plasmids

The vector pcDNA3.1-TMPRSS6, expressing the wild type TMPRSS6 ORF fused to the FLAG epitope at the C-terminus and the vector pcDNA3.1-mycHJV expressing the human HJV cDNA in fusion with the myc epitope were kindly provided by C. Camaschella [13].

The vector pcDNA3-HJV was created by cloning the PCR-amplified HJV ORF into the HindIII/EcoRI sites of the pcDNA3 vector. The HJV cDNA was PCR-amplified from HUH-7 cell derived template cDNA by using the following primers:

HJV-F: CCCAAGCTTATGGGGGAGCCAGGCCA

HJV-R: CCCGAATTCTTACTGAATGCAAAGCCACAGAAC.

The vector pcDNA3.1-TMPRSS6(Y141C), expressing the Y141C mutated TMPRSS6 protein fused to the FLAG epitope at the C-terminus, was obtained using the “Gene Tailor Site-Directed Mutagenesis System” (Invitrogen) with the pcDNA3.1-TMPRSS6 as template and the primers:

Y141C-F: CTACAACCTCCAGCTCCGTCTGTTCCCTTTGGGGA

Y141C-R: AGACGGAGCTGGAGTTGTAGTAAGTTCCCA.

The vector for the minigene system, was generated by PCR amplification of 100ng patient genomic DNA using primers spanning from exon3 to exon5 within the TMPRSS6 gene and Pfu Ultra DNA polymerase (Stratagene):

ex3-F: AAAGAATTTCGGTACAAGGCGGAGGTGATG

ex5-R: AAACCTCGAGCCAGGATCACTAGGCCCTCG

The PCR fragment was restriction digested and cloned into the EcoRI/XhoI sites of the pcDNA3 vector (Invitrogen). The pEGFP-TMPRSS6 and pEGFP-TMPRSS6(Y141C) vectors were obtained by subcloning the coding sequence of TMPRSS6 from the pcDNA3.1-TMPRSS6 and pcDNA3.1-TMPRSS6(Y141C) to pEGFP-n1 using the HindIII restriction sites.

All the vectors were controlled via automatic sequencing performed by GATC-biotech (GATC biotech, Konstanz, CH).

Cell culture

The human hepatoma HuH-7 cell line and the human fibroblast HeLa cell line were cultured in DMEM high glucose with GlutaMAX (Invitrogen, Carlsbad, CA) supplemented with 10% heat-inactivated fetal bovine serum (Invitrogen, Carlsbad, CA), 100 U/ml penicillin, 100 µg/ml streptomycin and 1mM Sodium pyruvate. The human hepatoma Hep3B cell line was cultured in EMEM medium supplemented with 10% fetal bovine serum, 1mM Sodium Pyruvate, 1mM Glutamine, 100 U/ml penicillin, 100 µg/ml streptomycin. Cells were maintained in 5% CO₂ atmosphere at 37°C. Cell transfections were performed by using the TransIT-LT1 Transfection Reagent (Mirus-bio) according to manufacturer's guidelines.

Microscopy

To analyze intracellular TMPRSS6 protein expression 150.000 HeLa cells were plated on 420mm² Lab-Tek Chambered Coverglass slides (Nunc, Denmark) and transfected with pEGFP-TMPRSS6 or pEGFP-TMPRSS6(Y141C). After 48h the medium was replaced by DMEM complete medium without red phenol and analyzed by live microscopy.

To analyze surface TMPRSS6 protein expression 150.000 HeLa cells were plated on a glass coverslip and transfected with pcDNA3.1-TMPRSS6 or pcDNA3.1-TMPRSS6(Y141C). After 48h the samples were fixed in 3% PFA, blocked with 1% BSA/0.3M Gly in PBS, incubated overnight at 4°C with an anti-FLAG (1:200 Sigma F3165) primary antibody and subsequently for 1h with an anti-mouse-FITC conjugated antibody (1:250, Sigma F5262). Cells were mounted on slides with mowiol and analyzed by microscopy. In both cases samples were visualized using a PerkinElmer Improvion Ultraview VoX Spinning disc confocal microscope and analyzed with Improvion Volocity 5.3.1 and ImageJ 1.42q.

RNA isolation and qRT-PCR

Total RNA was isolated using the Qiagen RNAeasy kit according to the manufacturer's instruction (Qiagen). One microgram of total RNA was reverse transcribed in a 25µl reaction using M-MLV reverse transcriptase (Fermentas) and random oligomers as primers. SYBR green Real-Time PCR was performed using the ABI StepONE Plus Real Time PCR System (Applied Biosystems) using the following primers:

hs_GAPDH-F: CATGAGAAGTATGACAACAGCCT

hs_GAPDH-R: AGTCCTTCCACGATACCAAAGT

hs_HAMP-F: CTCTGTTTTCCCACAACAGAC

hs_HAMP-R: TAGGGGAAGTGGGTGTCTC

Relative hepcidin mRNA expression was normalized to the GAPDH (glyceraldehyde-3-phosphate-dehydrogenase) mRNA. Results were calculated using the Pfaffl method [17].

Luciferase assay

Hep3B cells (95,000 cells) were plated per well in a 12 well plate. 24 h later the cells were transfected with 200ng of pGL3-hepcidin(WT_2.7Kb) reporter vector containing 2.7 kb of the 5'-flanking genomic region of the human hepcidin gene plus its 5'-UTR, 10ng of a control plasmid containing the Renilla gene under the control of the CMV promoter, 400ng of pcDNA3-HJV vector and 200ng of pcDNA3.1-TMPRSS6 or pcDNA3.1-TMPRSS6(Y141C). The next day cells were lysed in passive lysis buffer (Promega), and cellular extracts were analyzed for luciferase activity using the Dual-Luciferase-Reporter assay system (Promega) and a Centro LB 960 luminometer (Berthold Technologies, Bad Wildbad, Germany).

Immunoprecipitation assay

HeLa cells (2 millions) were transfected with 7.5µg of pcDNA3.1-mycHJV and with 7.5µg of pcDNA3.1-FLAG (mock) or 7.5µg of pcDNA3.1-TMPRSS6 or 7.5µg of pcDNA3.1-TMPRSS6(Y141C). After 24h cells were lysed in NET buffer (50mM Tris pH 7.4, 150mM NaCl, 5mM EDTA, 1% Triton X-100) supplemented with NaF, PIC, PSMF and Na₃VO₄. The lysate was incubated with 40µl of pre-equilibrated Anti-Flag M2 affinity gel (Sigma A2220) for 4h. Following 3 washing steps in NET buffer, samples were eluted in Laemmli loading buffer (62.5mM Tris pH 6.8, 2% SDS, 10% Glycerol, 0.1% 2-Mercaptoethanol, 0.0005% Bromophenol blue) and the eluted proteins were separated on a 10% SDS-PAGE for western blotting. Immunorecognition was performed by using an anti-FLAG (Sigma F7425) or an anti c-Myc polyclonal antibody (Sigma C3956).

Analysis of TMPRSS6 autocatalytic cleavage

HeLa cells (2.2 millions) were seeded on a 10cm dish and transfected with 15µg of pcDNA3.1-TMPRSS6, 15µg of pcDNA3.1-TMPRSS6(Y141C) or 15µg of pcDNA3.1-FLAG (mock) using the TransIT-LT1 Transfection Reagent (Mirus-bio) in DMEM complete medium. The next day cells were washed with PBS and the medium was exchanged with serum-free OPTImem (GIBCO) with or without 0.1mM β-mercaptoethanol, to create a reduced environment. 12h later the supernatant was collected and concentrated using Amicon Ultra 3k Centrifugal Filter (Millipore) (90min, 4°C, 4000g). The cells were lysed in NET buffer supplemented with NaF, PIC, PSMF and Na₃VO₄. Protein concentrations were determined by the BCA assay (Pierce). Fifty micrograms of total protein extract or of concentrated supernatant were separated on a 10 % SDS-PAGE and transferred to a Protran BA83 nitrocellulose membrane. Monoclonal anti-tubulin (SIGMA T5168), anti FLAG (SIGMA F7425), anti-mouse peroxidase conjugated (Sigma A9044) and anti-rabbit peroxidase conjugated (Sigma A0545) were used for immunorecognition.

Bioinformatic analysis

Sequence alignment of the SEA domain was performed by ClustalW (EBI; www.ebi.ac.uk/clustalw/). The sequences were retrieved from the Genbank database using the following accession numbers: Homo sapiens: NP_705837; Pan troglodites: XR_024662; Rattus norvegicus: NP_001124028; Mus musculus: NP_082178; Canis familiaris: XP_531743; Macaca mulatta: XP_001085319; Monodelphis domestica: XP_001376304 and from the ENSEMBL database with the following accession numbers: Pongo pygmaeus: ENSPPYP00000013149; Cavia porcellus: ENSCPOP00000004089; Ornithorhynchus anatinus: ENSOANP000000021472.

The ribbon structure was obtained by using the "Crystal Structure Of Sea Domain Of Transmembrane Protease From Mus Musculus" (PDB ID: 2E7V) as structural template and readapted using the swiss-prot DeepView program version 4.0.1.

Results:

Patient clinical synopsis

Our patient is the second son of healthy, non-consanguineous parents from Lebanon. Hematological disorders have not been reported in his family. In his second year of age, microcytic, hypochromic anemia was diagnosed. Subsequent iron supplementation did not improve his haematological parameters. As a 10-year-old boy his family moved to Germany and he was referred to our pediatric hematology department because of chronic weakness, occasional bone pain, and extensive sleeping. His physical strength and fitness were normal and he attended a regular school. He ate normal varied food and had normal appetite and stool. He had not suffered from infection or fever in recent months. Body weight was in the normal range between the 10th and 25th percentile but his height has dropped just below the 3rd percentile. The laboratory parameters showed a persistent decrease of haemoglobin (7.9 to 9.4 g/dl), erythrocyte number (4.82 to $5.5 \times 10^6/\mu\text{l}$), Mean Corpuscular Volume (59.8 to 62.5 fl), and Mean Corpuscular Hemoglobin (16.4 to 17.7 pg). Reticulocytes and other blood cell counts were within the normal range with the exception of thrombocytes which sometimes were increased with a maximum of $548,000/\mu\text{l}$. We found normal serum liver and renal parameters including normal total protein and albumin. Analysis of iron metabolism parameters showed normal values for serum ferritin, transferrin and iron binding capacity. By contrast, transferrin saturation (4.8 to 3.3 %) and serum iron levels (12 to 18 $\mu\text{g/dl}$) were pathologically low, while serum transferrin receptor levels (4.77 to 5.03 $\mu\text{g/dl}$) and zinc protoporphyrin in erythrocytes (332 to 378 $\mu\text{mol/mol}$ hemoglobin, normal < 40) were significantly increased. Bone marrow cytology showed normal blast numbers, erythropoiesis and megakaryopoiesis, both with discrete dysplastic features, and granulopoiesis. Iron staining discovered a clear lack of iron in macrophages. The bone marrow cytogenetic findings were normal. Pathologically low ^{59}Fe incorporation is the finding from scintigraphic examination, and this finding corresponds with the clinical observation of non-effective iron supplementation.

The haematological data collected from the proband are summarized in table 1.

Urinary hepcidin levels are elevated in the IRIDA patient

Hypochromic, microcytic anemia with low transferrin saturation that cannot be treated by iron supplementation is a strong indication for IRIDA. Since this disorder is hallmarked by increased hepcidin expression we analysed urinary hepcidin levels in the patient compared to four age-matched male healthy donors. The amount of the 25-aa mature hepcidin peptide (Hamp-25) was analyzed using a SELDI-TOF mass spectrometry assay and CM10 ProteinChip-arrays [16]. Hepcidin levels were normalized against creatinine (Fig. 1). The data show severely increased (15-fold) hepcidin levels in the patient urine, supporting the diagnosis of IRIDA.

c.442A>G, a novel mutation in the 4th exon of TMPRSS6

To PCR amplify all 18 TMPRSS6 exons and exon/intron boundaries PCR primers were designed within intronic sequences. Sequence analysis of the PCR products failed to detect any *TMPRSS6* mutation previously associated with IRIDA. Instead, we identified a homozygous nucleotide exchange (c.442A>G) within exon 4 which, together with exons 3 and 5, constitutes the SEA domain. To exclude hemizygoty of the allele we also sequenced the 4th exon of *TMPRSS6* of both parents. As shown in figure 2, a heterozygous c.442A>G base substitution was detected in both parents clearly indicating that the mutation was homozygous in the patient.

Mutations in *ALAS2*, *MFRN2* (*SLC25A28*) and *SLC11A2* (*DMT1*) were excluded in previous analysis. Within the *SLC11A2* gene a heterozygous SNP in intron 5 (IVS5+60 C>T) was detected. Genetic haemoglobin analysis discovered a heterozygote $\alpha^{3.7}$ -globin gene deletion which resulted in an α^+ -thalassemia trait.

TMPRSS6 c.442A>G does not affect splicing of exon4

The novel c.442A>G mutation within exon 4 of the *TMPRSS6* gene is located 10 nucleotides from the 3' end of the exon and substitutes the codon triplet TAT to TGT. This raises the possibility that the newly formed GT sequence could act as an aberrant "splice donor" that may trigger incorrect splicing between the fourth and fifth exon leading to a premature termination of the *TMPRSS6* protein.

Because *TMPRSS6* expression is restricted to liver tissue [9] a splicing defect cannot be investigated by mRNA analysis of patient blood cells. We therefore designed a minigene that spans exon 3 to exon 5 (including intron 3 and 4) of the *TMPRSS6* gene containing the c.442A>G mutation to transfect HeLa cells. As shown in figure 3, this minigene construct is correctly spliced suggesting that the c.442A>G mutation is unlikely to cause aberrant splicing.

TMPRSS6(Y141C) impairs TMPRSS6 maturation:

The c.442A>G base substitution exchanges tyrosine with cysteine at amino acid 141 within the SEA (Sea urchin sperm protein, Enteropeptidase, Agrin) domain of *TMPRSS6*. Phylogenetic sequence analysis of the *TMPRSS6* protein indicates that amino acid residue 141 is highly conserved suggesting that this tyrosine may be important for *TMPRSS6* function (Fig. 4a). Introduction of an additional cysteine within the second β -sheet of the SEA domain (Fig. 4b) may interfere with secondary structure formation of *TMPRSS6*, a protein that already contains 37 cysteines. We therefore next assessed whether the *TMPRSS6*(Y141C) mutation causes protein mislocalization. *TMPRSS6*(Y141C) or *TMPRSS6* protein fused to the EGFP protein was expressed in HeLa cells and the fluorescent signal was analyzed by confocal microscopy. As shown in figure 5a, both the overexpressed wild-type and mutant *TMPRSS6* proteins localize predominantly in intracellular compartments (e.g. the endoplasmic reticulum). To assess membrane localization of *TMPRSS6*, HeLa cells were transfected with *TMPRSS6* or *TMPRSS6*(Y141C), both C-terminally fused with a FLAG epitope that is predicted to be located in the extracellular space. The cells were analyzed by immunocytochemistry using primary anti-FLAG and secondary FITC-conjugated antibodies on fixed, non-permeabilized cells. As shown in figure 5b, both the *TMPRSS6* and *TMPRSS6*(Y141C) proteins localize to the cell surface, suggesting that faulty processing and localization of the *TMPRSS6* mutant protein does not explain IRIDA in the patient.

TMPRSS6 was shown to control hepcidin mRNA expression by binding and proteolytically cleaving HJV [18]. To assess whether amino acid residue 141 of *TMPRSS6* is critical for binding HJV we next transfected HeLa cells with a myc-tagged HJV fusion construct alone or together with plasmids coding for *TMPRSS6* or *TMPRSS6*(Y141C) proteins both tagged with a FLAG epitope. Immunoprecipitation of *TMPRSS6* or *TMPRSS6*(Y141C) using anti-FLAG antibodies both detects HJV protein at the expected molecular weight of 55KDa (Fig. 6a, lanes 2 and 3). No signal is detected in the sample transfected with HJV and a control vector (Fig 6a, lane 1). This experiment demonstrates that the Y141C mutation does not affect binding to HJV.

TMPRSS6, like other serine proteases, is auto-activated by proteolytic cleavage within a RIVGG motif at its pro-domain/catalytic domain junction site. Once cleaved, the 30KDa catalytic domain remains attached to the rest of the protein via a disulfide bridge. HeLa cells were transfected with a control plasmid or with plasmids coding for *TMPRSS6* or *TMPRSS6*(Y141C). Subsequently, both the cell lysates as well as the concentrated medium supernatant were analyzed for *TMPRSS6* expression by western blotting. Interestingly, only conditioned medium (CM) from cells transfected with *TMPRSS6* plasmid revealed a *TMPRSS6* protein fragment of around 30kD which corresponds to the expected size of the catalytic domain (cd*TMPRSS6*) (Fig. 6b, lane 2). A similar fragment failed to be detected in cells transfected with the *TMPRSS6*(Y141C) (Fig. 6b, lane 3) or control vectors (Fig. 6b, lane 1), despite efficient expression of the *TMPRSS6*(Y141C) protein as detected in the cell lysate (CL) (Fig. 6b, middle panel). Analysis of equal protein amounts was assured by detection of tubulin (Fig. 6b, lower panel).

A lack of cdTMPRSS6 in the conditioned medium of TMPRSS6(Y141C)-transfected cells may either indicate a lack of proteolytic auto-activation of the mutated protein or increased binding stability of the catalytic domain to the rest of the protein due to the formation of an extra disulfide bond in the Y141C mutated protein.

In an attempt to distinguish between these two possibilities, we repeated the experiment but added the reducing agent β -mercaptoethanol (0.1mM) to the cell culture medium. As shown in figure 6c (upper panel – lanes 3 and 4) HeLa cells transfected with TMPRSS6(Y141C) fail to release cdTMPRSS6 into the medium, both under regular and reducing conditions. By contrast, cdTMPRSS6 is readily detected under both conditions in cells transfected with the wild-type construct (Fig 6c). Efficient protein expression of TMPRSS6 and the mutant form are monitored in the cell lysate (Fig. 6c, lower panel).

Taken together these data support the interpretation that TMPRSS6(Y141C) fails to be auto-activated by proteolytic cleavage.

TMPRSS6(Y141C) over expression increases hepcidin mRNA expression

TMPRSS6(Y141C) leads to the synthesis of an inactive form of TMPRSS6. To assess whether this defect affects hepcidin mRNA expression, we next transfected the human hepatoma cell line Hep3B with a firefly luciferase reporter vector under the control of the full length hepcidin promoter together with expression vectors coding for HJV and TMPRSS6 or TMPRSS6(Y141C) proteins. Firefly luciferase activity was normalized with renilla luciferase under the control of a constitutive CMV promoter.

As expected, transfection of the HJV expression vector results in a 3.5 fold increase of luciferase activity. Cotransfection with TMPRSS6 completely abolished this effect. Importantly, cotransfection of TMPRSS6(Y141C) only slightly attenuated the HJV-controlled hepcidin response, resulting in a 2-fold hepcidin promoter activation (Fig.7a). Similar findings were obtained analyzing endogenous hepcidin mRNA levels (Fig.7b), suggesting that the amino acid substitution at position 141 is sufficient to inhibit HJV-controlled hepcidin activation and thus likely explains the IRIDA phenotype.

Discussion:

We report the clinical case of a 10-year old boy with IRIDA hallmarked by microcytic, hypochromic anemia that could not be resolved by iron administration. Iron treatment likely was ineffective as a consequence of high hepcidin levels in the blood reflected by increased urinary hepcidin excretion (Fig. 1), which block duodenal iron uptake and macrophage iron release [19]. Sequence analysis detected a homozygous mutation (c.422A>G) within the fourth exon of the TMPRSS6 gene (Fig. 2). We initially hypothesized that substitution of the codon triplet TAT to TGT may generate an additional 'splice donor' sequence. However, a transfected minigene containing the mutation was accurately spliced between the fourth and fifth exon (Fig. 3), suggesting that an amino acid substitution of tyrosine to cysteine at aminoacid 141 may affect TMPRSS6 function. The mutation is located within the SEA domain of TMPRSS6 which is predicted to be localized within the extracellular part of the TMPRSS6 protein. A SEA domain is also present in the Enteropeptidase, another TTSP family member, in all of the HAT/DESC subfamily proteins and in the closely related Matriptase and Matriptase-3 [20]. The biological role of this domain remains to be determined. In some proteins the SEA domain is subject to autoproteolysis causing the production of a soluble form of the protein that is released from the cell surface. Such an autoproteolytic event can be accelerated by conformational stress within the SEA domain itself [21]. Cleavage occurs between glycine and serine within a conserved GSVVV (mucin), GSVIV (enteropeptidase) or GSVIA (matriptase) motif [21-23]. It is not yet clear if the

SEA domain of the human TMPRSS6 is also subject to autoproteolysis. Analysis of the primary amino acid sequence failed to detect a common cleavage motif identifying only as putative GSLRV motif.

The TMPRSS6(Y141C) protein localizes to similar subcellular regions like the wild-type TMPRSS6 protein (Fig. 5), suggesting that selective retention of TMPRSS6(Y141C) protein within the cytoplasm does not occur. Immunoblotting of medium supernatant of TMPRSS6(Y141C) and TMPRSS6 transfected cells failed to detect the entire extracellular domain of the TMPRSS6 protein as a consequence of cleavage within the SEA domain contrasting data by Ramsay and collaborators that detect fragments of the appropriate size in both wild-type and mutant TMPRSS6 proteins.

So far, it is not clear which protein domain of TMPRSS6 binds to HJV and vice versa. Here we show that the TMPRSS6(Y141C) mutation does not affect co-immunoprecipitation with HJV, suggesting that the interaction domain may be localized within other domains of TMPRSS6.

Finally, we show that the Y141C amino acid substitution affects the maturation of the TMPRSS6 protein. TMPRSS6 is initially synthesized as an inactive proenzyme that upon auto-activation cleaves the C-terminal catalytic domain within the RIVGG consensus sequence. The cleaved domain remains attached to the rest of the protein via a disulfide bond. Western blot analysis (under reducing conditions) of tissue culture medium from cells transfected with TMPRSS6 revealed a 30KDa fragment that corresponds in size to the activated catalytic domain of the TMPRSS6 protein. In addition, we detected a minor 60KDa fragment that has previously been proposed to represent a dimeric form of the catalytic domain [18]. Interestingly, both the 30kDa and the 60kDa fragments were undetectable in TMPRSS6(Y141C) transfected cells. It is unlikely that the additional cysteine in TMPRSS6(Y141C) may have stabilized the interaction between the cdTMPRSS6 and the rest of the protein, because addition of β -mercaptoethanol to the cell culture medium did not result in the detection of cdTMPRSS6 upon expression of TMPRSS6(Y141C) (Fig. 6c). Our data thus suggest that the tyrosine residue at amino acid 141 likely is required for TMPRSS6 autocatalytic cleavage. TMPRSS6 auto-activation is critical for protein function because transfection of TMPRSS6(Y141C) fails to attenuate hepcidin promoter activity (Fig.7). As a consequence hepcidin levels will be increased (Fig.1) and IRIDA will develop.

Interestingly, an additional mutation in the SEA domain (A118D) was recently shown to be critical for TMPRSS6 auto-activation [15]. It is thus intriguing to speculate that the SEA domain could act as a scaffold structure that maintains TMPRSS6 folding in order for auto-activation to occur. Substitution of tyrosine with an additional cysteine within the second β -sheet of the SEA domain (Fig. 4b) may interfere with the formation of disulfide-bridges within TMPRSS6, a protein that already contains 37 cysteines. Alternatively, the mutation could affect N-linked glycosylation of the SEA domain that may affect protein stability.

Together with other data our results suggest that unprocessed TMPRSS6(Y141C) still reaches the cell surface, interacts with HJV but fails to cleave HJV. As a consequence the BMP/SMAD4 signalling pathway is hyperactive resulting in excess hepcidin transcription. Functional characterization of the TMPRSS6(Y141C) thus gives novel insight into understanding TMPRSS6 function and pathogenesis of IRIDA.

References:

- 1 Buchanan, G. R. and Sheehan, R. G. (1981) Malabsorption and defective utilization of iron in three siblings. *J Pediatr.* **98**, 723-728
- 2 Melis, M. A., Cau, M., Congiu, R., Sole, G., Barella, S., Cao, A., Westerman, M., Cazzola, M. and Galanello, R. (2008) A mutation in the TMPRSS6 gene, encoding a transmembrane serine protease that suppresses hepcidin production, in familial iron deficiency anemia refractory to oral iron. *Haematologica.* **93**, 1473-1479

- 3 Andrews, N. C. (1997) Iron deficiency: lessons from anemic mice. *Yale J Biol Med.* **70**, 219-226
- 4 Pearson, H. A. and Lukens, J. N. (1999) Ferrokinetics in the syndrome of familial hypoferremic microcytic anemia with iron malabsorption. *J Pediatr Hematol Oncol.* **21**, 412-417
- 5 Brown, A. C., Lutton, J. D., Pearson, H. A., Nelson, J. C., Levere, R. D. and Abraham, N. G. (1988) Heme metabolism and in vitro erythropoiesis in anemia associated with hypochromic microcytosis. *Am J Hematol.* **27**, 1-6
- 6 Finberg, K. E., Heeney, M. M., Campagna, D. R., Aydinok, Y., Pearson, H. A., Hartman, K. R., Mayo, M. M., Samuel, S. M., Strouse, J. J., Markianos, K., Andrews, N. C. and Fleming, M. D. (2008) Mutations in *TMPRSS6* cause iron-refractory iron deficiency anemia (IRIDA). *Nat Genet.* **40**, 569-571
- 7 Folgueras, A. R., de Lara, F. M., Pendas, A. M., Garabaya, C., Rodriguez, F., Astudillo, A., Bernal, T., Cabanillas, R., Lopez-Otin, C. and Velasco, G. (2008) Membrane-bound serine protease matriptase-2 (*Tmprss6*) is an essential regulator of iron homeostasis. *Blood.* **112**, 2539-2545
- 8 Du, X., She, E., Gelbart, T., Truksa, J., Lee, P., Xia, Y., Khovananth, K., Mudd, S., Mann, N., Moresco, E. M., Beutler, E. and Beutler, B. (2008) The serine protease *TMPRSS6* is required to sense iron deficiency. *Science.* **320**, 1088-1092
- 9 Velasco, G., Cal, S., Quesada, V., Sanchez, L. M. and Lopez-Otin, C. (2002) Matriptase-2, a membrane-bound mosaic serine proteinase predominantly expressed in human liver and showing degrading activity against extracellular matrix proteins. *J Biol Chem.* **277**, 37637-37646
- 10 Ramsay, A. J., Reid, J. C., Velasco, G., Quigley, J. P. and Hooper, J. D. (2008) The type II transmembrane serine protease matriptase-2--identification, structural features, enzymology, expression pattern and potential roles. *Front Biosci.* **13**, 569-579
- 11 Hooper, J. D., Campagnolo, L., Goodarzi, G., Truong, T. N., Stuhlmann, H. and Quigley, J. P. (2003) Mouse matriptase-2: identification, characterization and comparative mRNA expression analysis with mouse hepsin in adult and embryonic tissues. *Biochem J.* **373**, 689-702
- 12 Nemeth, E., Tuttle, M. S., Powelson, J., Vaughn, M. B., Donovan, A., Ward, D. M., Ganz, T. and Kaplan, J. (2004) Heparin regulates cellular iron efflux by binding to ferroportin and inducing its internalization. *Science.* **306**, 2090-2093
- 13 Silvestri, L., Guillem, F., Pagani, A., Nai, A., Oudin, C., Silva, M., Toutain, F., Kannengiesser, C., Beaumont, C., Camaschella, C. and Grandchamp, B. (2009) Molecular mechanisms of the defective hepcidin inhibition in *TMPRSS6* mutations associated with iron-refractory iron deficiency anemia. *Blood.* **113**, 5605-5608
- 14 Lee, P. (2009) Role of matriptase-2 (*TMPRSS6*) in iron metabolism. *Acta Haematol.* **122**, 87-96
- 15 Ramsay, A. J., Quesada, V., Sanchez, M., Garabaya, C., Sarda, M. P., Baiget, M., Remacha, A., Velasco, G. and Lopez-Otin, C. (2009) Matriptase-2 mutations in iron-refractory iron deficiency anemia patients provide new insights into protease activation mechanisms. *Hum Mol Genet.* **18**, 3673-3683
- 16 Altamura, S., Kiss, J., Blattmann, C., Gilles, W. and Muckenthaler, M. U. (2009) SELDI-TOF MS detection of urinary hepcidin. *Biochimie.* **91**, 1335-1338
- 17 Pfaffl, M. W. (2001) A new mathematical model for relative quantification in real-time RT-PCR. *Nucleic Acids Res.* **29**, 2002-2007
- 18 Silvestri, L., Pagani, A., Nai, A., De Domenico, I., Kaplan, J. and Camaschella, C. (2008) The serine protease matriptase-2 (*TMPRSS6*) inhibits hepcidin activation by cleaving membrane hemojuvelin. *Cell Metab.* **8**, 502-511
- 19 Muckenthaler, M. U. (2008) Fine tuning of hepcidin expression by positive and negative regulators. *Cell Metab.* **8**, 1-3
- 20 Bugge, T. H., Antalis, T. M. and Wu, Q. (2009) Type II transmembrane serine proteases. *J Biol Chem.* **284**, 23177-23181

- 21 Macao, B., Johansson, D. G., Hansson, G. C. and Hard, T. (2006) Autoproteolysis coupled to protein folding in the SEA domain of the membrane-bound MUC1 mucin. *Nat Struct Mol Biol.* **13**, 71-76
- 22 Matsushima, M., Ichinose, M., Yahagi, N., Kakei, N., Tsukada, S., Miki, K., Kurokawa, K., Tashiro, K., Shiokawa, K., Shinomiya, K. and et al. (1994) Structural characterization of porcine enteropeptidase. *J Biol Chem.* **269**, 19976-19982
- 23 Cho, E. G., Kim, M. G., Kim, C., Kim, S. R., Seong, I. S., Chung, C., Schwartz, R. H. and Park, D. (2001) N-terminal processing is essential for release of epithin, a mouse type II membrane serine protease. *J Biol Chem.* **276**, 44581-44589

Figure legends:

Table 1. Hematological parameters. An asterisk indicates pathological values. MCH, mean corpuscular haemoglobin content; MCV, mean corpuscular volume; Hb, hemoglobin

Figure 1. Elevated urinary hepcidin levels in the IRIDA patient. Urine was analyzed from the IRIDA patient and 4 healthy age-matched male volunteers (Ctrl) by SELDI-TOF-MS applying CM10 ProteinChips. Hepcidin arbitrary intensity units were normalized to creatinine.

Figure 2. Family pedigree. Sequence analysis of the TMPRSS6 gene indicates heterozygosity for the novel c.442A>G mutation in both parents and homozygosity for the same mutation in the affected proband (marked by an arrow).

Figure 3. c.442A>G base substitution does not affect splicing. A minigene spanning exons 3 to 5 of the TMPRSS6 gene was transfected in HeLa cells. Correct splicing between exon 4 and exon 5 was detected by sequence analysis of the resulting cDNA. The c.442A>G mutation is indicated by an asterisk. The sequence in capital letters indicates the sequence of the minigene. The sequence in lower case represents the sequence of the wild-type TMPRSS6 cDNA (accession number NM_153609).

Figure 4. The tyrosine residue at position 141 is highly phylogenetically conserved A) Alignment of the TMPRSS6 SEA domain. Tyrosine 141, the only cysteine located in the SEA domain and aminoacid residues that represent putative glycosylation sites are shown in bold. B) Ribbon structure of the human SEA domain of TMPRSS6 generated by adaptation of the crystal structure of the SEA domain of the murine TMPRSS11d transmembrane protease (2E7V). The localization of tyrosine 141 within the second β -sheet of this domain is indicated.

Figure 5. TMPRSS6 and TMPRSS6(Y141C) localize to similar subcellular regions. A) Localization of transfected TMPRSS6-EGFP and TMPRSS6(Y141C)-EGFP in HeLa cells by live confocal microscopy. B) Cell surface expression of TMPRSS6-Flag and TMPRSS6(Y141C)-Flag in transiently transfected HeLa cells. Cells were fixed without permeabilization and membrane proteins were detected using an anti-FLAG antibody. Signal detection by confocal microscopy.

Figure 6. TMPRSS6(Y141C) binds HJV but fails to auto-catalytically activate itself. A) HeLa cells were transfected with plasmids expressing HJV-myc or pcDNA3.1-FLAG (mock), TMPRSS6-Flag or TMPRSS6(Y141C)-Flag as indicated. After TMPRSS6 immunoprecipitation using an anti-Flag antibody (IP α FLAG), TMPRSS6 and the TMPRSS6-bound HJV were immunorecognized by western blotting using an anti-FLAG antibody (WB α Flag) or an anti-myc antibody (WB α myc)

respectively. B) HeLa cells were transfected with pcDNA3.1-FLAG (mock), TMPRSS6-Flag or TMPRSS6(Y141C)-Flag. Following 24h in serum-free medium, the conditioned medium (CM) was collected, concentrated and analyzed for the presence of the proteolytic TMPRSS6 fragments by western blotting. C) HeLa cells were transfected with TMPRSS6-Flag or TMPRSS6(Y141C)-Flag, washed and incubated with serum-free OPTImem (GIBCO) with or without 0.1mM β -mercaptoethanol (β -ME) for 12 hours. The conditioned medium was collected, concentrated and analyzed by western blotting for cdTMPRSS6. Effective TMPRSS6 transfection was assessed in the cell lysate (CL).

Figure 7. TMPRSS6(Y141C) expression fails to efficiently suppress hepcidin promoter activity. A) Luciferase assay. The reporter plasmid pGL3-hepcidin(WT_2.7Kb) was transfected with either HJV alone or together with TMPRSS6 or TMPRSS6(Y141C) in Hep3B cells. 24h later, luciferase activity was measured and normalized against renilla luciferase. Results are presented as fold change \pm SD of the transfected cells and compared to cells transfected only with the reporter construct (WT_2.7Kb). B) qRT-PCR assay. Hep3B cells were transfected with either HJV alone or together with TMPRSS6 or TMPRSS6(Y141C). 24h later, total RNA was extracted. Hepcidin mRNA expression was analyzed by quantitative real time PCR and normalized to GAPDH. Results are presented as fold change \pm SD.

Acknowledgments:

S.A. is funded by the Medical Faculty of Heidelberg. M.U.M. acknowledges funding of eRARE-BMBF (HMA-IRON). The authors wish to thank M. Hentze for helpful discussions.

	Patient value	Normal range
Ferritin	86 ng/ml	17-105 ng/ml
Transferrin	262 mg/dl	210-315 mg/dl
Iron*	12-18 µg/dl	92-184 µg/dl
Transferrin saturation*	3,3-4,8%	15-45%
Soluble Tf receptor*	4,77-5,03 µg/dl	0,83-1,76 µg/dl
MCV*	59,8-62,5 fl	83-97 fl
MCH*	16,4-17,7 pg	28-34 pg
Hb*	7,9-9,4 g/dl	14-18 g/dl
Zinc Protoporphyrin (ZPP)*	378,2 µmol/mol Heme	<40

Table 1

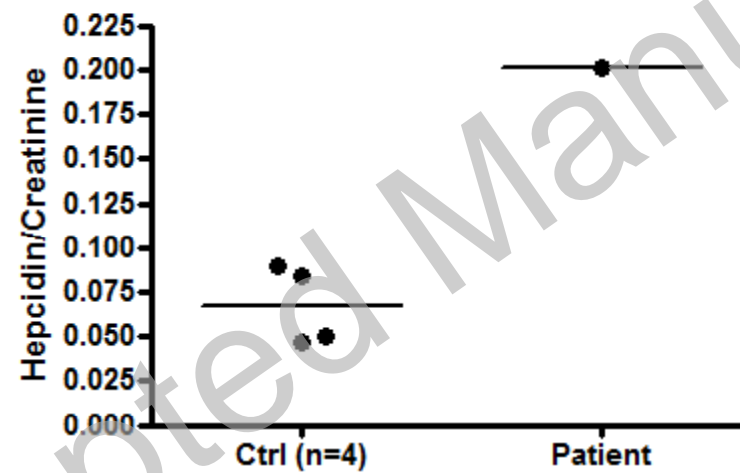


Figure 1

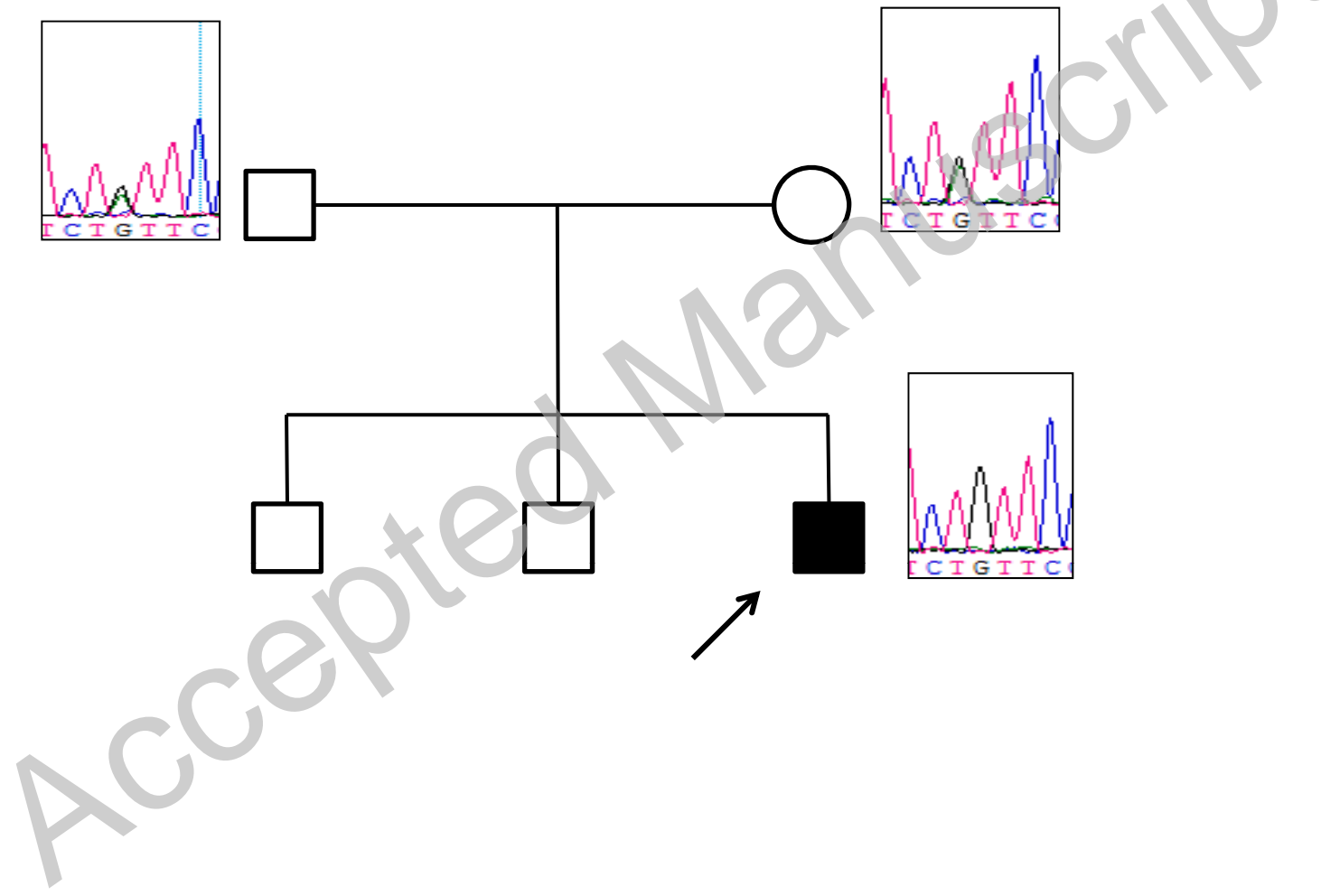


Figure 2

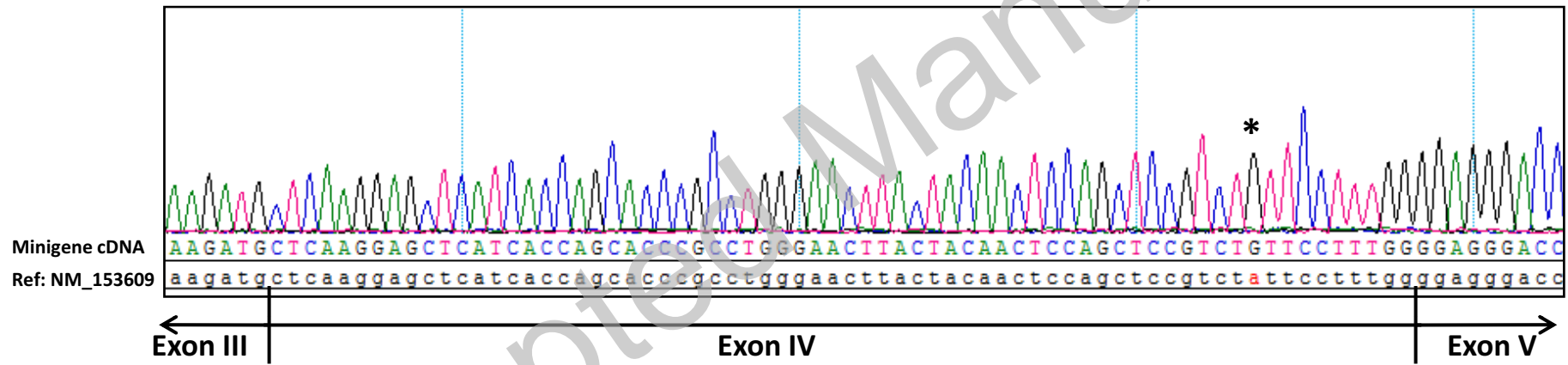


Figure 3

A

Homo sapiens	MVSQVYSGSLRVLNRHFSQDLTRRESSAFRSETAKAQKMLKELITSTRLGTYYNSSSVY ¹ SFGEGPLTCFFWFILQIPEHRRMLMSPEVVQALLVEELLSTVNSS
Pan troglodites	TVSQVYSGSLRVLNRHFSQDLTRRESSAFRSETAKAQKMLKELITSTRLGTYYNSSSVY ¹ SFGEGPLTCFFWFILQIPEHRRMLMSPEVVQALLVEELLSTVNSS
Pongo pygmaeus	TVSQVYSGSLRVLNRHFSQDLTRRESSAFRSETAKAQKMLKELITSTRLGTYYNSSSVY ¹ SFGEGPLTCFFWFILQIPEHRRPMLSPEVVQALLVEELLSTVNSS
Macaca mulatta	TVSQVYSGSLRVLNRHFSQDLTRRESSAFRSETAKAQKMLKELIASTRLGTYYNSSSVY ¹ SFGEGPLTCFFWFILQIPEHRRMLMSPEVVQALLVEELLSTVNSS
Mus musculus	TVSQVYSGSLRVLNRHFSQDLGRRESIAFRSESAKAQKMLQELVASTRLGTYYNSSSVY ¹ SFGEGPLTCFFWFILDIPEYQRLTSPVVRELLVDELLS--NSS
Rattus norveg.	TISQVYSGSLRVLNRHFSQDLARRESIAFRSETAKAQKMFQELVASTRLGTYYNSSSIY ¹ AFGEGPLTCFFWFILDIPEYQRLTSPVVRELLVDELLS--NSS
Cavia porcellus	TVSQVYAGSLRVLNRHFSQDLARRESSIFRSESAKAQKMLRELITSTRLGTHYNSSSVY ¹ AFGEGPLTCFFWFILKIPEHLQPTLSPVMRVLLVEELLTAANAS
Canis famil.	TVSQVYSGSVRVLNRHFSQDLARRESSAFRSETAKAQKMLKELIASTRLGTYYNSSSVY ¹ SFGEGPLTCFFWFILQIPEHRRPMLSPEVVRALLVEELLSTANSS
Monodelphis dom.	TVSQLYSGSIRVLNRHFNLDSRRDSSAFRSETAKAQKMLRELIFTTRLAPYNSSTVY ¹ AFGEGPLTCFFWFILQIPESTRQTLTPEAVKEVLVERLLSNANET
Ornithorhynchus	TSSRLYSGSVAVLDQRQFFPDLANHESGAFRSEIAKAQIMLKELISATRLSAYNSSTVY ¹ SFGAKPLTCFFWFILQVPNSKVQKMSPDWVKEVLVDELKARANAS

SEA DOMAIN

B

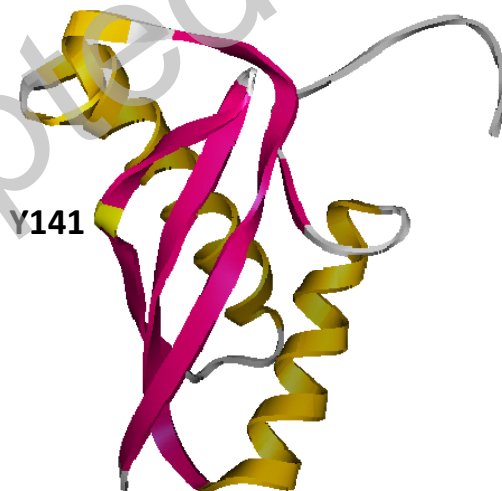


Figure 4

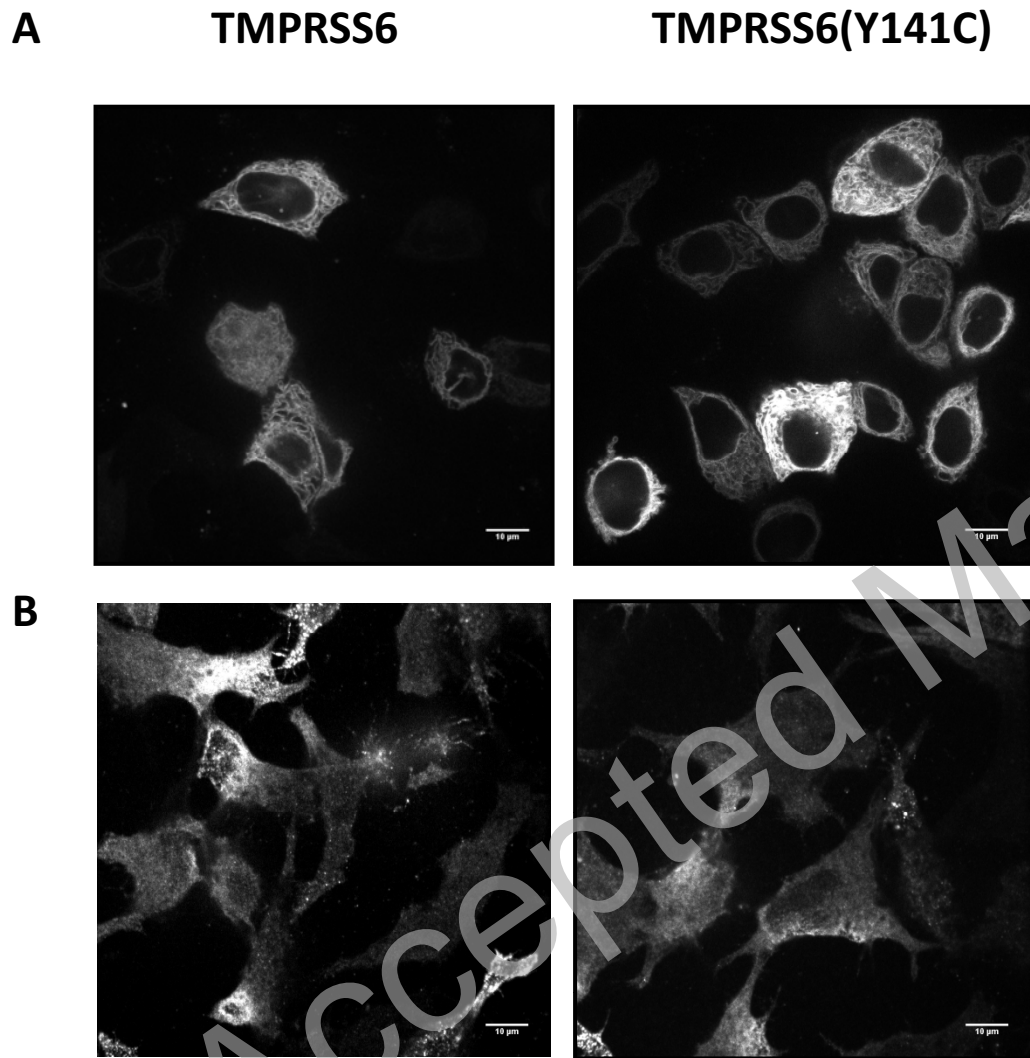


Figure 5

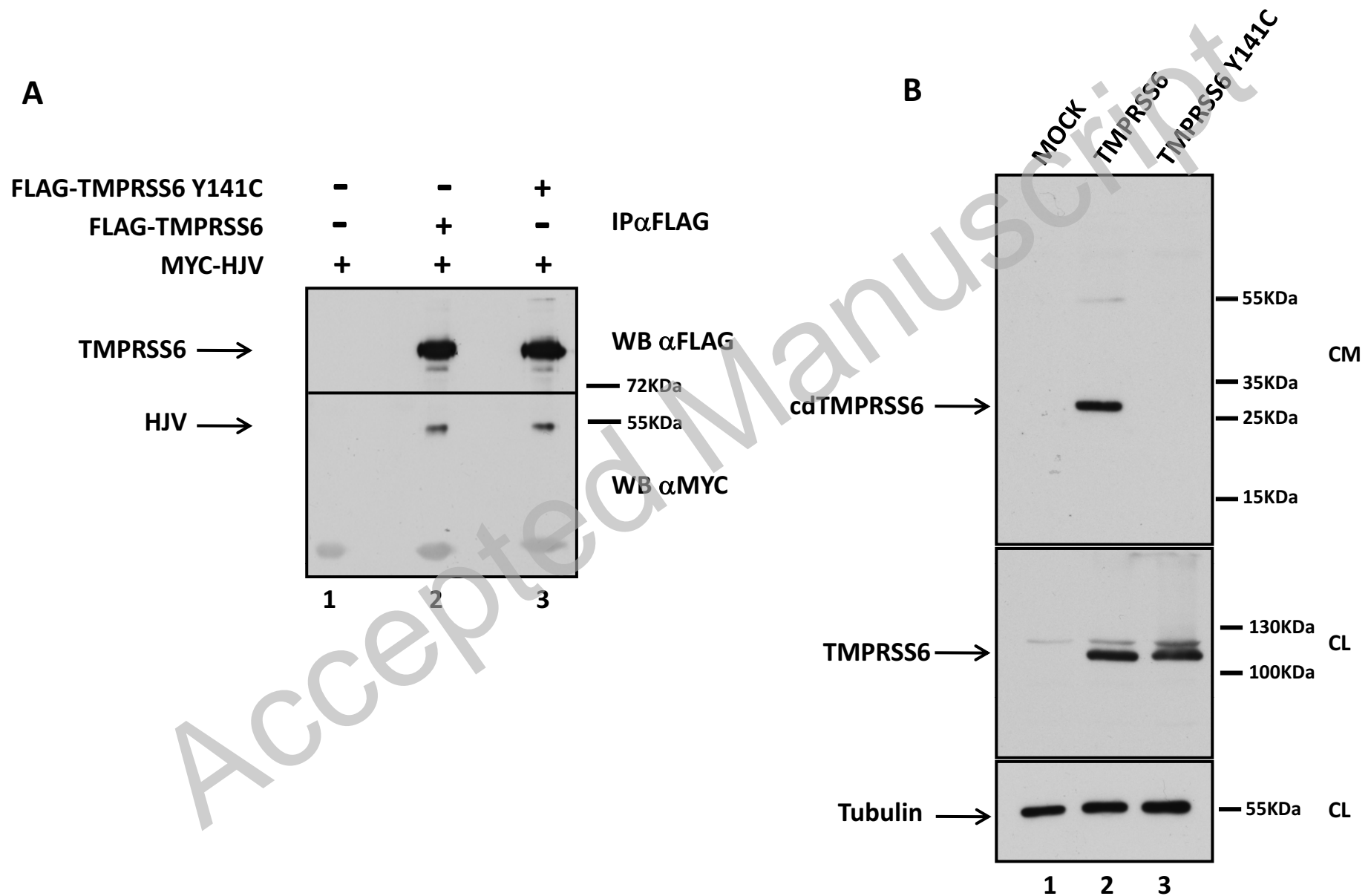


Figure 6

C

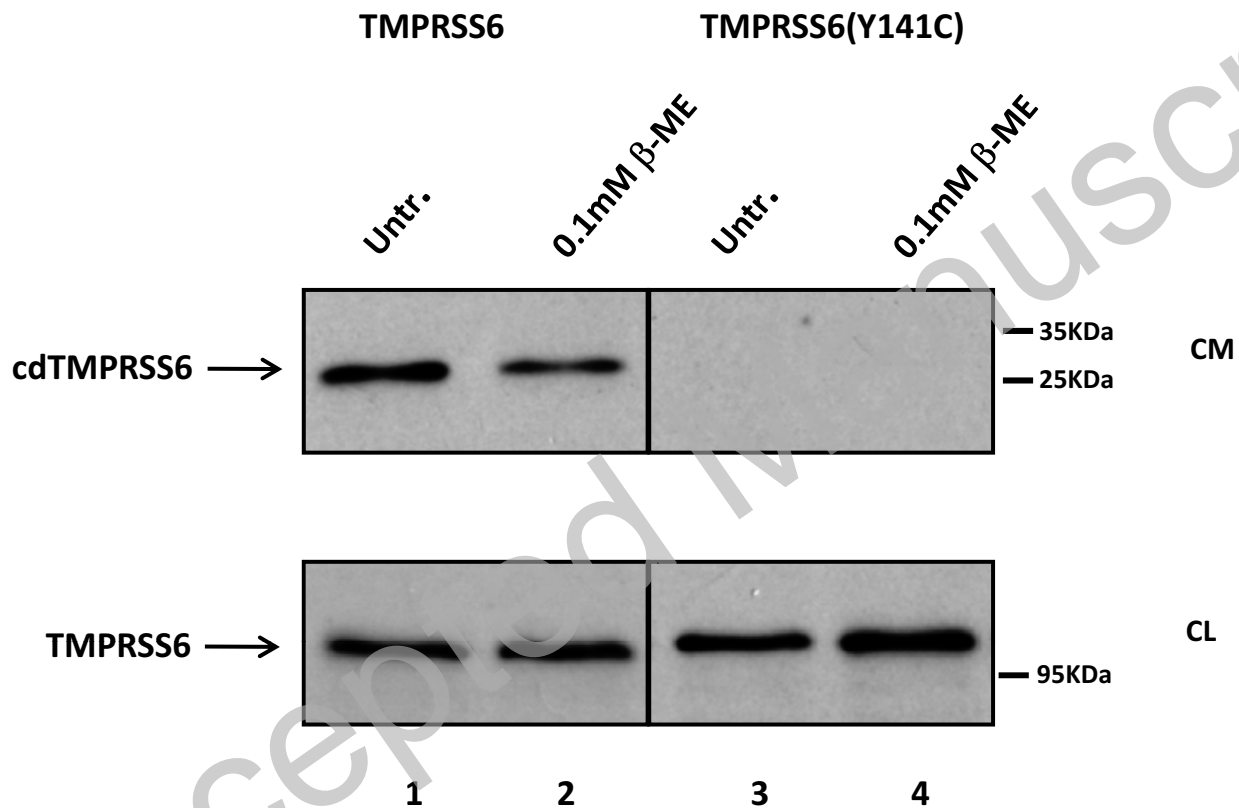


Figure 6

Licensed copy. Copying is not permitted, except with prior permission and as allowed by law.

© 2010 The Authors Journal compilation © 2010 Portland Press Limited

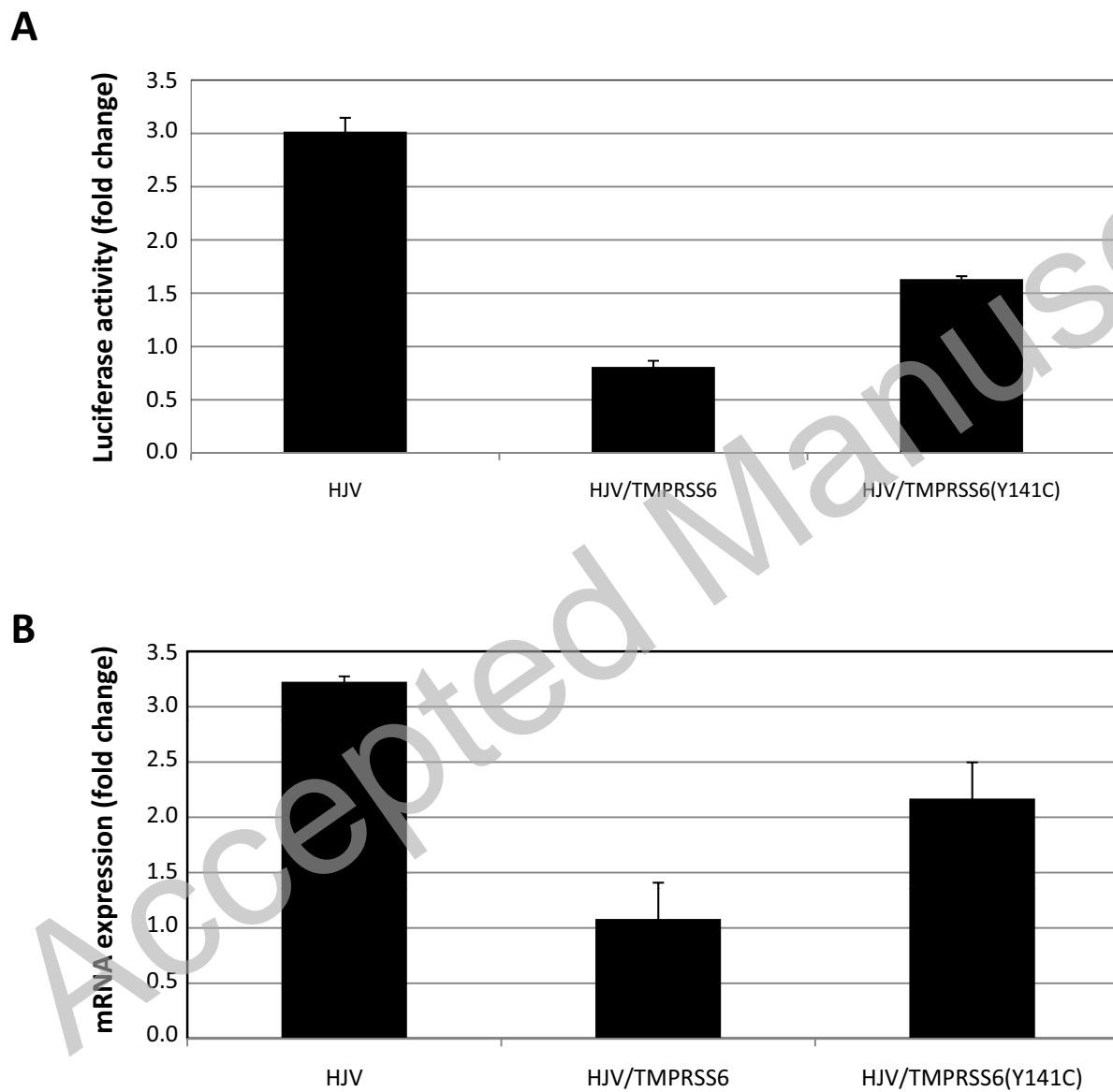


Figure 7